Pressure-Sensitive Sampling Wands for Homeland Security Applications

Matthew E. Staymates, Jessica Grandner, and Jennifer R. Verkouteren

Abstract—This paper discusses the use of force sensing resistor (FSR) technology integrated into sampling wands used for homeland security applications. FSR-integrated wands can be used for the optimization of wipe sampling of surfaces to facilitate enhanced trace contraband collection. Collection efficiencies during wipe sampling are known to be dependent on the applied force, or pressure, used during sampling. Light-emitting diodes designed to switch from red to green at a defined force threshold of 7 N provide feedback to the operator during sampling. The goal of maintaining forces at or above the threshold was successfully demonstrated by testing with a volunteer population of 22. An additional benefit is the reduction in the variability of the force applied by each operator during sampling. Another focus area is the development of prototype sampling wands that fit in the palm of the hand and other wand modifications that increase the reliability of wipe sampling by registering the placement of the collected sample properly on the wipe. This paper also outlines how an array-based FSR can be used to visualize contact area and pressure during wipe sampling.

Index Terms—Explosives, narcotics, particle collection, trace detection, wipe sampling.

I. INTRODUCTION

THE detection of trace explosives and narcotics has become a growing area of research and development within the scientific community, owing its status to the ever-increasing threat of terrorist activities around the world. Working with bulk contraband materials (*i.e.*, creating improvised explosive devices or handling illicit narcotics) is expected to contaminate the body, clothing, and surrounding surfaces with micrometer-sized particles of the contraband material [1]. During security screening, one attempts to collect and interrogate a representative sample from a person or items they have handled, and detect the contraband if it is present. The low volatility of many explosives and narcotics limits the ability to detect molecular vapors [2] and so the primary focus is on collecting particles.

The collection of trace contamination can be accomplished by physically wiping a collection cloth across the surface.

This is a sampling approach employed in many fields in addition to homeland security screening, including environmental, nuclear, and industrial hygiene monitoring. There are many factors that affect collection efficiency during wipe sampling, as reviewed in an earlier study conducted by one of the authors [3]. Notable among these is the applied force or pressure used during sampling. The earlier study demonstrated that for the range of forces expressed by human operators when asked to sample with "firm" force, a linear increase in collection efficiency with force was observed. Sample collection efficiency is key to improving the probability of detection in an explosive trace detector (ETD). It was determined that operator performance could be modified through feedback from a force-sensing resistor (FSR) used to measure forces during sampling. FSRs are polymer thick-film devices that show a decrease in resistance with an increase in the force applied to the active surface.

One notable difference in wipe sampling for trace explosives, as opposed to other fields, is the use of a sampling wand to hold the collection cloth or wipe, rather than using the hand. The wand allows the operator to have standoff distance from the object, and protects the operator from potential harm when reaching into suitcases, etc. Another significant difference is the requirement to focus the collected material to a limited area of the wipe, consistent with the area of the thermal desorber in the ETD. The collection wipe is inserted into the instrument, where it is rapidly heated to temperatures exceeding 200 °C to convert the particles to vapors. The heated area of the wipe is typically a small portion of the total wipe area, and any particles collected outside the heated zone are not likely to be detected. This means that the wand must focus the collection of particles to a specific area of the wipe, which we refer to as the "sweet spot".

A sampling wand with an integrated FSR can serve two functions—to provide feedback to the operator during sampling that sufficient force is applied and to ensure that the force is directed in the correct location. Here, we describe the integration of single element FSRs directly into the sampling wands, with feedback to the operator provided by light emitting diodes(LEDs) triggered at defined force thresholds. The goal here is to compel a user to push with a force above a certain threshold. In addition, we demonstrate how array-based FSRs can be used to provide critical feedback in wand design by imaging the contact area with respect to the sweet spot of the wipe. We also present designs for FSR-integrated sampling wands that take into account some of the unique functional requirements of current ETDs.
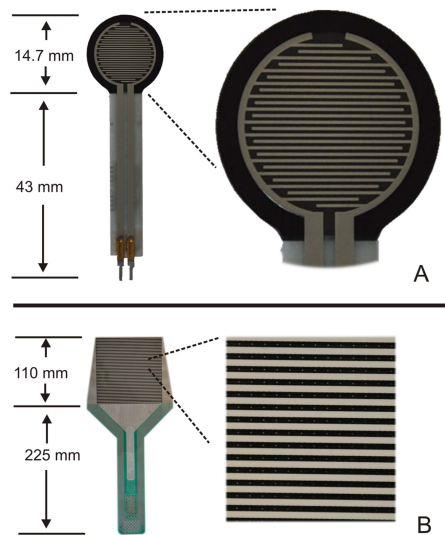
Fig. 1. Image of the single-element FSR (A) and the array-based FSR (B) used in this study. The active area of the FSR has been magnified to show the interdigitated elements of the conductive electrodes.
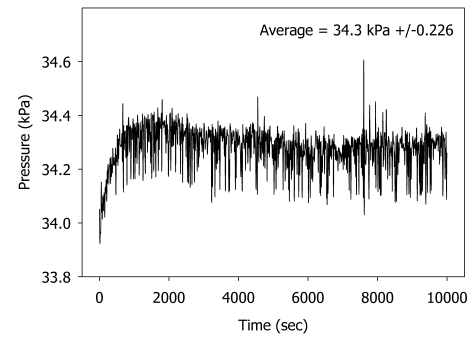

Fig. 2. Pressure fluctuation of the FSR response measurement system. 34.4 kPa of pressure is applied to each FSR as a function of time for 2.8 hours.

II. FLEXIBLE FORCE SENSING RESISTORS

The single-element FSRs used in this study are manufactured by Interlink Electronics (FSR model 402, Camarillo, CA) and have a 14.7 mm diameter active area. They consist of two layers of a polymer film substrate that are laminated together. The first layer contains interdigitating conductive electrodes and the second a semiconductive polymer. The FSR sustains an open circuit until force is applied to either side of the device. As force is applied, there is increased shunting of the conductive layer and FSR resistance declines [4]. The polymer is not infinitely compressible, so the conductance will saturate [5].

The array-based FSR used in this study is a Tekscan model 5101 for the I-Scan system (Tekscan Inc., South Boston, MA). The sensor has an active area of 110 mm by 110 mm, and each sensing element in the array (44×44) has a sampling area of 6.5 mm^2. This particular model has an applied pressure limit approaching 345 kPa and must be calibrated often because of drift that occurs in the sensor over time. The system allows for a two point calibration with loading values that should fall between 20% and 80% of the expected maximum loading. The calibration of this sensor is described in detail in [6]. Images of the single-element FSR and the array-based FSR are shown in Fig. 1.

III. RESPONSE MEASUREMENTS OF SINGLE ELEMENT FSRs

In order to evaluate the reliability of the single element FSRs for field settings, the repeatability, lifetime, and dynamic response under different loading configurations were tested. A unique measurement system was developed that consists of an inflatable bladder (PB100E Equilibration Device, Tekscan Inc.) that compresses a series of FSRs and measures their resistance as a function of applied force. Pressure is controlled from an electronic pressure regulator with closed loop feedback monitoring via pressure transducer. A data acquisition algorithm was created to collect resistance information for up to 16 FSRs at once. A data acquisition board from National Instruments collects resistance measurements from each FSR. The system can currently apply pressure up to 41 kPa (6 psi), but could be expanded to greater pressures. The force applied to each FSR can be calculated because the active area of the FSR is known.

Measuring FSR dynamic response is done by applying uniform pressure to the FSR for a set amount of time, and then releasing pressure from the FSR. The user can input the number of requested cycles, the amount of force applied to the FSRs, and the period at which the pressure cycles. For example, if the period is set to a total of 10 seconds, the pressure is applied for 5 seconds and released for 5 seconds, and then the cycle repeats. The data is automatically saved and the system shuts itself down once the experiment is over. The data acquisition code also records the pressure during each FSR measurement to ensure that the applied force is consistent throughout the experiment. Results of the applied pressure during a typical experiment are shown in Fig. 2.

It is clear that the pressure control in this system is sufficiently consistent. There exists a short warm-up period for the pressure controller to reach steady-state operation, but the difference in transient to steady-state pressures are on the order of hundredths of a kPa. The precise control over the pressure of this system offers great flexibility when measuring FSR response and repeatability.

Single element FSRs are known to be inherently non-linear in terms of response, and many researchers have developed algorithms to partially overcome nonlinearity, creep, and hysteresis associated with the FSR signal [7]–[9]. However, the single element FSRs used in these studies exhibited a response that was better than expected under dynamic compressive loading. Twenty different FSR sensors were tested with this bladder system, and the variability between sensors was found to be less than 10%. To determine the error associated with these FSRs, a 6th order polynomial function was used to predict the FSR response in real time. A polynomial regression algorithm calculates the constants in the 6th order polynomial and then immediately solves the equation based on the
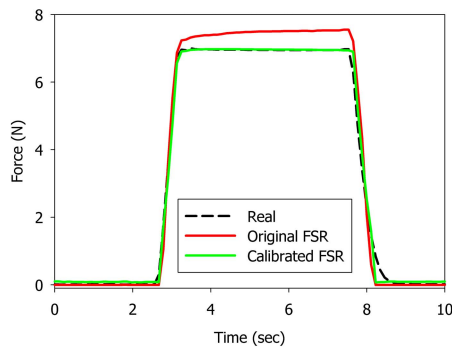
Fig. 3. FSR response under dynamic compressive loading for a calibrated and uncalibrated FSR.
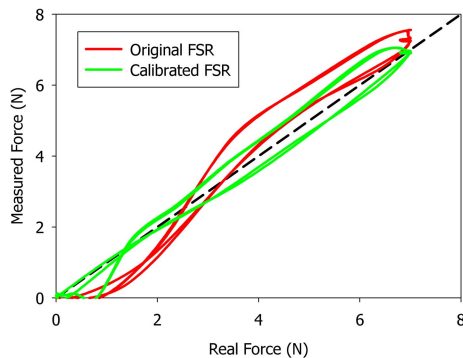

Fig. 4. Measured FSR force response compared to the dynamic compressive force for an original and a calibrated FSR. Here, the inflatable bladder was ordered to apply 7 N for 5 seconds, and then release.

resistance measured by the FSR. These constants are unique to each individual FSR because the properties of each are slightly different. Fig. 3 illustrates the moderate improvements that can be gained with the use of this algorithm. Data shown in Fig. 3 are results from a single FSR under dynamic compressive loading. In this example, the bladder is instructed to apply 7 N for 5 seconds, and then release. The original FSR that has not been calibrated has a response that closely matches the input loading. If the calibration algorithm is applied, the FSR output almost exactly matches the input loading.

During the initial spike in force that is applied by the inflatable bladder, the original FSR responds quickly and follows the true force quite accurately. However, the original FSR response demonstrates a moderate level of creep when the force is held constant at 7N. The calibrated signal from the FSR agrees with the real force throughout the entire dynamic loading event, except near the trailing edge of the plot.

Fig. 4 shows a graph of the real force vs. the measured force for both the original and the calibrated FSR response. The dashed line with a slope on unity represents a perfect system that exhibits no hysteresis or creep because the relationship between real and measured force is one to one. The data reveal that the original, uncalibrated FSR shows an offset from the idealized line. The calibrated FSR response line has been shifted and closely matches the idealized line. Note that the hysteresis and creep have not been completely eliminated, but small improvements can be made to these low-cost flexible sensing devices by incorporating relatively simple algorithms

into the data acquisition circuitry. The purpose of this error analysis and FSR calibration is to ensure that response of the non-linear FSR is as close as possible to the real force being applied to a surface.

IV. FORCE THRESHOLD

The FSR, when integrated into a sampling wand, will have a force threshold that defines when to switch an LED from red to green. This threshold must be based on what is practical to expect a human operator to attain, and what results in improved sample collection. In the earlier study, we determined that a random population asked to sample with "firm" force would apply an average force of 7 N. [3]. There were significant differences in applied force among the 20 participants, and one force is unlikely to be comfortable for all. In addition, the participants used a sampling wand approximately 30 cm in length. The length of the wand and/or the placement of the hand on the wand defines the moment arm experienced by the wrist, and differences in length may affect the force that operators are comfortable in applying. Determining some average "firm" force that suits everyone may not be possible, and we chose to use 7 N as a starting value. An increase in collection efficiency with increasing force was reported in the earlier paper from sampling 10 μm fluorescent microspheres. To confirm that this applied to explosive particles, we repeated the study using the explosive compound hexahydro-1,3,5-trinitro-1,3,5-triazine (RDX). Samples containing a known amount of RDX were prepared and transferred to flat, vinyl test surfaces with a dry-transfer method outlined in [10]. In this technique, solutions containing the explosive analyte are deposited onto non-wetting surfaces, in this case a foil-backed Teflon film (Bytac bench and shelf protector, SPI, West Chester, PA) and allowed to dry. The dry deposits are transferred to the test surface by rubbing. For these experiments, the solutions were dispensed using drop-on-demand inkjet printing to deposit volumes of approximately 0.001 μL, which resulted in RDX particles approximately 20 μm in diameter [11]. The mass of explosive material used in these experiments is at a challenge level for the ETD instrument.

Once RDX particles were transferred to the test surfaces, wipe collection was performed at three nominal forces, 1 N, 4 N, and 7 N, within a 10 cm by 10 cm area. Three different commercially-available ETDs with their associated wands and collection wipes were used, and alarm rates were determined for 10 replicates at each nominal force. The results are shown in Fig. 5 and indicate that the alarm rate positively correlates with the sampling force for each ETD system. The data were also evaluated in terms of the RDX peak intensities with respect to saturated instrument values, which is one component of the alarm rate and a measure of collection efficiency. The data evaluated in this manner exhibit the same trends shown in Fig. 5.

V. INTEGRATION INTO SAMPLING WANDS

Our first integrated FSR wand was created by using the existing commercial wand for the Itemizer DX benchtop ETD
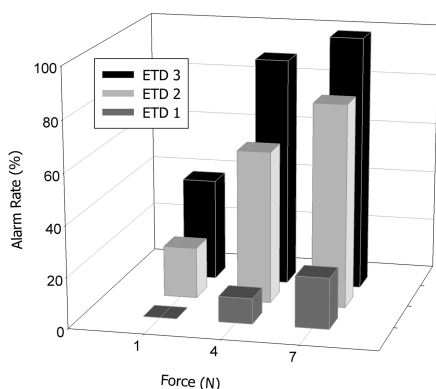
Fig. 5. Alarm rates for three different ETDs from sampling a fixed amount of RDX at three nominal forces. Alarm rates based on 10 replicates at each nominal force.

TABLE I
WIPING FORCES WITH AND WITHOUT AN INTEGRATED FSR

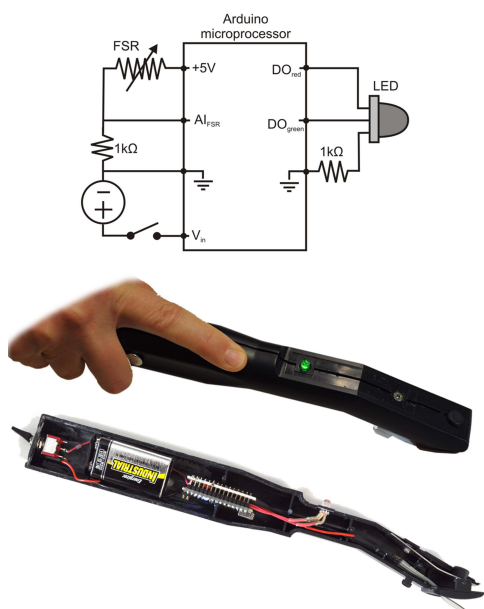|	Standard Wand		FSR Wand	
	"Firm" force *		7 N Threshold	
Operator	Average (N)	SD	Average (N)	SD
1	5	0.9	7.6	0.8
2	5.3	0.8	9	0.8
3	5.4	1.2	6.7	0.9
4	5.4	1	8.5	0.7
5	6	1.7	8	1.1
6	11.4	2.4	8.5	1.1
7	13.4	2.4	9.4	0.7

*Data from [3]

Fig. 6. Schematic diagram of the electronic circuit used in the prototype FSR wand. The LED used in this design is a multi-color LED that contains both red and green colors. An image of the internal components of the wand and an image of the final assembly are also shown.

(Morpho Detection, Newark CA). The body of the wand is hollow and has ample room for the electronics needed to monitor the FSR and control the LED. The flexible FSR is mounted to the wand body in a location that is directly under the contact area of the swab. A photograph of the FSR wand, along with a schematic diagram of the electronic circuit is shown in Fig. 6.

An Arduino microprocessor (Arduino Nano, www.arduino.cc) was used to handle all functions of the FSR wand. As shown in Fig. 6, a 9VDC battery is used to supply power to the device. 5V is supplied to the FSR, which has a resistance that varies from several megaohms under no force down to hundreds of ohms under maximum allowable force. A 1 kΩ pull-down resistor creates a voltage divider circuit to ensure that the current flowing through the FSR is minimized.

A code was written in the native Arduino language and uploaded to the microprocessor. This code is executed in real-time by the on-board processor and does not require external control or communication with a computer to operate. The calibration correction algorithm discussed in the previous section was not included in the overall code because these FSRs are not being used for quantitative measurements of force and it was determined that they perform at an acceptable level without the calibration.

When the prototype FSR is activated, the microprocessor begins monitoring the voltage at AI_{FSR} (see Fig. 6) and the red LED is illuminated by the digital output line DO_{red}. The voltage at AI_{FSR} begins to rise as the wand is being wiped across a surface and force is applied to the FSR. Once the voltage crosses a specified threshold, output to the DO_{red} stops and DO_{green} begins. The LED turns green and the user has a visual indication that sufficient force is being applied to the surface. The FSR sampling wand was placed in a special mounting system that is positioned above an analytical balance to verify that the threshold setpoint matched the target value.

The target threshold was set at 7 N, and the operation of the wand was evaluated by recording forces with the array FSR during sampling experiments. Some of the participants of the previous study that used a standard wand were asked to participate in this study using the new FSR-integrated wand. Each person was asked to sample as before within a 10 cm by 10 cm area on the array FSR using a continuous S-shaped pattern to fill the area (see [3] for details). The participants were asked to keep the light green during sampling and were encouraged to practice prior to testing. Forces were recorded at 10 Hz, initiating collection at first contact and ending at last contact. The average and standard deviation were calculated as given in Table 1 and compared to previous data for each participant.

The integrated sensor resulted in average forces higher than 7 N for each operator, except for one, and reduced the variation in force from an average of 20% relative standard deviation (RSD) to 11% RSD. Because there is no light indicating excessive force, participants were free to use as much force as possible to keep the light green. This resulted in an average force using the FSR-integrated wand of 8.2 N,
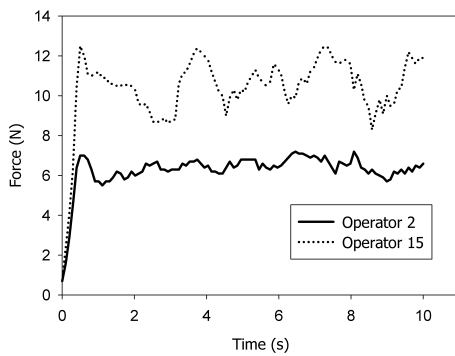
Fig. 7. Example of two different operators attempting to maintain a green light while sampling a surface with the FSR wand. The green light transition was set to 6N. Without the feedback of a green light, applied force varies upwards of 20% on average. With the integration of an FSR in the sampling wand, the user variability is reduced to about 11% on average.
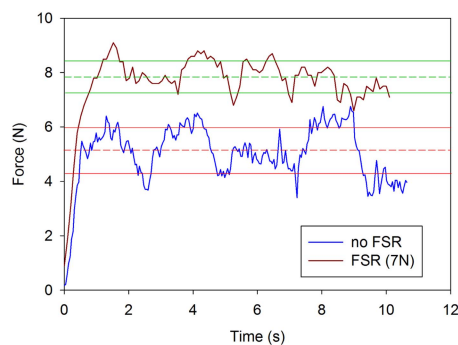

Fig. 8. Example of the applied force of one operator using a sampling wand with and without an FSR. The dashed lines of each trace represent the average of that trace, and the solid horizontal lines are one standard deviation from the average.

TABLE II

WIPING FORCES WITH FSR WAND GREEN-LIGHT
THRESHOLD SET AT 6N

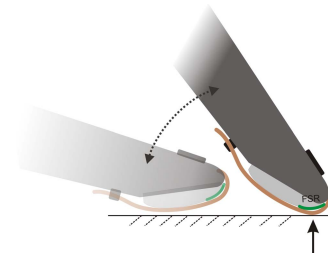| Operator	Average (N)	SD
1	5.8	0.7
2	6.5	0.4
3	6.9	0.9
4	7.1	0.6
5	7.2	0.6
6	7.3	1.2
7	7.3	1.1
8	7.6	1
9	8.4	0.9
10	8.9	1.2
11	9.1	1
12	9.7	1.2
13	9.8	1.2
14	10.7	1.8
15	10.8	1.2

Fig. 9. Schematic diagram of the tip of a wand that illustrates how the FSR can be employed as an angle indicator as well as a force indicator. If the wand is held at an angle outside of the intended range, then the FSR senses zero force and the LED turns red.

given a 7 N threshold. An additional 15 participants were then asked to use the FSR-integrated wand with a threshold set at 6 N (Table 2). The majority of participants again exceeded the force threshold, although the range includes forces near the threshold up to almost 5 N over the threshold (Fig. 7). The variability within each experiment averaged 12% RSD, which again is a considerable reduction in variability compared to the use of a regular wand without an integrated FSR. Only one of the 22 operators felt that the 7 N threshold was difficult to attain, and that they experienced discomfort in applying this level of force. These results are of course limited to the study participants, and a larger survey would be required to determine whether this firm force threshold is comfortable for a target population of screeners.

Fig. 8 shows the applied force of a single operator with and without an integrated FSR in the sampling wand. Over a 10s sampling time, the minimum force without the FSR is about 3N compared to a minimum of 6.5N with the integrated FSR. The addition of an FSR in the sampling wand has kept the average variability down, raised the average applied force, and restricted the minima to near the threshold. To improve explosives detection, our primary goal is to ensure that the applied force used is consistently above 7 N, and so achieving a limiting threshold and a reduction in variability are both important and have been demonstrated in these experiments.

Based on the results, we would recommend setting the threshold value to 7 N.

The integrated FSR provides a second benefit in addition to visual confirmation that sufficient force is being applied. This particular wand has a rounded backing surface for the wipe that allows the contact area to move along a rocking direction based on the angle of the wand. The sweet spot for particle collection is obtained for a limited range of rocking angles, and in this case the FSR also acts as an angle indicator. Fig. 9 shows a schematic diagram that illustrates how the FSR functions as an angle indicator as well as a force indicator. The FSR is represented as a green line and is located near the sweet-spot of the wipe.

VI. IMAGING WAND CONTACT AREA

Although design limitations such as the variable contact area described above can be overcome by integrated FSRs, it is best to design the wand to function correctly under normal usage. Array-based FSRs can be very helpful in this regard, providing essential information to improve wand design. For maximum collection efficiency, the wand should focus the collection of particles to completely utilize the sweet spot of the wipe. This requires an even force distribution over the area of the sweet spot, which is usually accomplished by using a
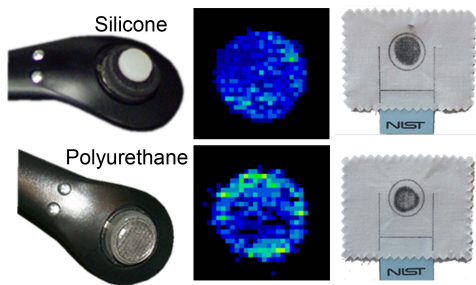
Fig. 10. ETD wand with two different types of attached bumpers (left), with pressure distributions imaged by FSR array (center), and resultant particle collection on wipes (right).
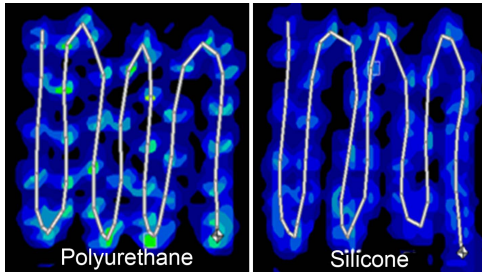

Fig. 11. Center-of-force lines (white) and pressure distributions (0 kPa – 96 kPa) from sampling with polyurethane and silicone rubber bumper attachments.
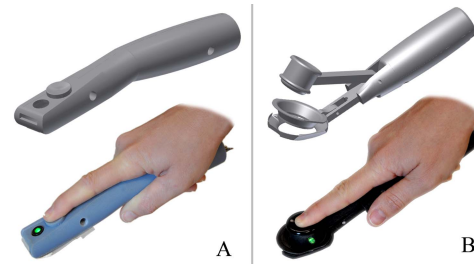

Fig. 12. Two prototype palm wands used for surface sampling. The top images show computer aided design (CAD) models while the bottom images show functioning prototype versions. The palm wand in (A) is designed for an Itemizer DX and the palm wand in (B) is designed for a 500DT made by Smiths Detection (Montreal Canada).

conformable surface, such as a rubber or polymeric material, as the backing behind the wipe. The pressure distributions produced by different surfaces attached to the wand and under normal usage can be imaged and related to the potential for particle collection.

For example, two different discs, or bumpers, of either silicon rubber (durometer hardness of 45 – 50) or polyurethane (durometer hardness of 60 – 70) are shown attached to an ETD wand in Fig. 10. These bumpers sit behind the cotton wipe, shown on the right in Fig. 10, with the "sweet spot" in the area defined by the circular marking on the cloth. The pressure distributions made by the bumpers at forces used in wipe sampling are shown in the center in Fig. 10.

The harder polyurethane bumper has high pressure regions on the perimeter and very little contact in the interior, while the softer silicone rubber bumper has a more homogeneous pressure distribution. Particle collection was evaluated by wipe sampling over a piece of carbon paper, and the distributions are qualitatively the same as the pressure distributions for the two bumpers. The differences in the pressure distributions of the two bumpers during wipe sampling are indicated in Fig.11, where sampling was conducted in a serpentine pattern over a 10 cm by 10 cm area at approximately 4 N of force. The polyurethane bumper caused the wand to be held at an angle to the surface, resulting in crescent-shaped pressure distributions. This results in a "snowplow" effect, where particle collection builds up on a leading edge, overwhelming the collection ability of that limited area of the wipe. The silicone bumper is naturally easier to hold flat against the surface, and the full area of the wipe corresponding to the sweet spot is available for particle collection. Fig. 11 demonstrates how array-based FSRs

can be used to visualize the force and pressure distributions of various sampling wand designs.

VII. Summary and Future Directions

The work presented here has demonstrated the efficacy of flexible FSRs to several Homeland Security applications, particularly wipe-based sampling of contraband material from surfaces.

The non-linear behavior of FSRs under dynamic loading conditions was observed with a unique measurement system that uses an inflatable bladder to apply uniform pressure to the active area of FSRs. This system was also be used to evaluate different calibration algorithms that attempt to correct for nonlinear FSR response.

Integration of FSR technology into wipe sampling wands was facilitated by the use of a microprocessor, a battery, and a multi-color LED. This LED is red when insufficient force is being applied by the user. When the integrated FSR senses 7 N of force, the LED turns green and the user has a visual indication that sufficient force is being applied to the surface. The 7 N threshold was based on improved ETD detection and human factors (the average "firm" force that people can apply routinely). The FSR-integrated wand was tested using 22 volunteers, and was found to provide sufficient feedback to allow the users to maintain average forces at, or above, the threshold. An additional benefit of the FSR feedback is the reduction in force variability during sampling. Also mentioned was the ability of the integrated FSR to act as an angle indicator. This helps to ensure that material collected during wipe sampling is concentrated in the sweet spot of the collection wipe.

The dynamic forces applied to a surface during wipe sampling were imaged with an array-based FSR. The influences of simple wand modifications, such as the addition of rubber bumpers, were visualized with the Tekscan system. The effects of these bumper modifications on pressure distribution were shown to be qualitatively related to a potential increase in particle collection.

Along with demonstrating the successful integration of FSR sensing technology into commercially-available trace sampling wands, we are developing novel sampling wands with an unconventional form factor. These new sampling wands are called "palm wands", as they are shaped and sized to fit in

the palm of the hand of the user. This concept of a short handheld wand has generated interest with our stakeholders and within the trace detection community. By positioning the hand closer to the wipe contact area and shortening the moment arm experienced by the wrist, we expect that the user will feel more comfortable while applying adequate force during surface sampling. Two examples of a palm wand are shown in Fig. 12.

An FSR and all associated circuitry shown in Fig. 6 have been incorporated into these palm wands. The bodies of these wands were created with an Objet 30 3D printer (Objet Inc., Billerica, MA). This 3D printer uses an inkjet printing approach to create physical models out of a plastic resin material. The resin, initially in a liquid state, is deposited drop-by-drop in 16 μm thick layers by a series of inkjet nozzles. This resin is a photopolymer that hardens in the presence of ultraviolet light. Once a layer of liquid resin is deposited, a high-intensity ultraviolet light bombards the surface and cures the layer. Another layer is then deposited and the process is repeated. A gel-like support material is deposited in locations where future voids will exist. This support material is manually removed with a high-velocity water jet once the build is complete.

This additive manufacturing technology offers many advantages for wand prototyping and facilitates rapid turnaround during development of new wand designs. While it is unclear if the FSR wands and palm wands will be adopted for use in a checkpoint environment, we do anticipate their use as training tools for stakeholders that use trace detection technologies.

Next steps in this work will include pilot studies with other federal agencies that utilize trace explosives and narcotics detection systems. Array-based FSR technology is expected to be a helpful training tool that allows users to visualize their wiping performance while they participate in wipe sampling exercises. The feasibility of FSR wands and palm wands in an operational setting is uncertain and will be evaluated in pilot programs. However, it is anticipated that these new prototypes will be a favorable addition to the current training protocols already in place for wipe sampling end-users.

ACKNOWLEDGEMENT

REFERENCES

[1] J. R. Verkouteren, "Particle characteristics of trace high explosives: RDX and PETN," *J. Forensic Sci.*, vol. 52, no. 2, pp. 335–340, 2007.

[2] B. Dionne, D. Rounbehler, E. Achter, J. Hobbs, and D. Fine, "Vapor pressure of explosives," *J. Energetic Mater.*, vol. 4, pp. 447–472, 1986.

[3] J. R. Verkouteren, N. W. M. Ritchie, and G. Gillen, "Use of force-sensing array films to improve surface wipe sampling," *J. Environ. Sci., Process. Impacts*, vol. 15, no. 2, pp. 373–380, 2013.

[4] Interlink Electronics. (2012, Oct.). *Force Sensing Resistor Integration Guide and Evaluation Parts Catalog*, Camarillo, CA, USA [Online]. Available: http://IEFSR.com

[5] E. Zehr, R. Stein, T. Komiyama, and Z. Kenwell, "Linearization of force sensing resistors (FSR's) for force measurement during gait," in *Proc. IEEE 17th Annu. Conf. Eng. Med. Biol.*, vol. 2. Sep. 1995, pp. 1571–1572.

[6] J. Brimacombe, D. Wilson, A. Hodgson, K. Ho, and C. Anglin, "Effect of calibration method on Tekscan sensor accuracy," *J. Biomech. Eng.*, vol. 131, no. 3, pp. 034503-1–034503-4, 2009.

[7] N. Rana, "Application of force sensing resistor (FSR) in design of pressure scanning system for plantar pressure measurement," in *Proc. 2nd Int. Conf. Comput. Electr. Eng.*, vol. 2. Dec. 2009, pp. 678–685.

[8] J. Florez and A. Velasquez, "Calibration of force sensing resistors (FSR) for static and dynamic applications," in *Proc. IEEE ANDESCON Conf.*, Sep. 2010, pp. 1–6.

[9] R. Hall, G. Desmoulin, and T. Milner, "A technique for conditioning and calibrating force-sensing resistors for repeatable and reliable measurement of compressive force," *J. Biomech.*, vol. 41, no. 16, pp. 3492–3495, 2008.

[10] R. Chamberlain, "Dry transfer method for the preparation of explosives test samples," U.S. Patent 6 470 730, Oct. 29, 2002.

[11] J. R. Verkouteren and J. Grandner, "Force dependent collection of explosives by wipe sampling," Mater. Meas. Lab., NIST, Gaithersburg, MD, USA, Tech. Rep. 637-30-12, Jul. 2012.

Matthew E. Staymates, photograph and biography is not available at the time of publication.

Jessica Grandner, photograph and biography is not available at the time of publication.

Jennifer R. Verkouteren, photograph and biography is not available at the time of publication.